Directional Etching Formation of Single-Crystalline Branched Nanostructures: A Case of Six-Horn-like Manganese Oxide

Xi-Guang Han, Ming-Shang Jin, Qin Kuang,* Xi Zhou, Zhao-Xiong Xie,* and Lan-Sun Zheng

State Key Laboratory for Physical Chemistry of Solid Surfaces and Department of Chemistry, College of Chemistry and Chemical Engineering, Xiamen University, Xiamen, 361005, People's Republic of China

Received: October 21, 2008; Revised Manuscript Received: December 8, 2008

In this paper, we successfully synthesized six-horn-like branched MnO nanocrystals by thermal decomposition of $Mn(CH_3CO_2)_2 \cdot 4H_2O$ in the present of 1-octylamine/oleic acid (OA) at 400 °C for 30 min. SEM and TEM observation indicate that every horn of six-horn-like MnO nanocrystals is constructed with a bundle of nanorods growing along the [100] direction. Adequate evidence provided by time- and temperature-dependent experiments demonstrates that the formation of such branched MnO can be divided into two processes, i.e., the formation of octahedron-based MnO exposed with polar surfaces and sequent directional etching. In this mechanism, the mixed solvent of organic amines and OA provides favorable circumstances for the formation of MnO octahedra, and at the same time, OA as the etching reagent is responsible for the evolution of six-horn-like MnO from octahedron-based MnO.

1. Introduction

In the past years, branched nanostructures have attracted increasing interest because of some interesting physical or chemical properties and potential applications resulting from their special three-dimensional (3D) structure.[1−13] To acquire various branched nanostructures, many synthetic strategies have been developed up to now. Multistep synthetic strategy is the most popular in the fabrication of branched nanostructures built with different materials. In this strategy, the growth of the secondary material is always determined by the position of the catalysts and the lattice match degree between the substrate and branched stem.[1−5] In addition, on the basis of the polytypism of crystal structure, some materials are also able to form homogeneous branched structures. Typically, AB compounds of groups II−VI (A = Zn, Cd; B = O, S, Se, and Te) can grow into a tetrapod-like structure where the core belongs to the zinc-blende structure but four legs belong to the wurtzite structure.[6−10] In the case of a homogeneous or heterogeneous system, the formation of such 3D branched nanocrystals is closely related to the characteristic of the crystal structures of these materials.

Manganese(II) oxide (MnO), a common metal oxide with a cubic structure, has attracted more attention as a model system for the theoretical study of electronic and magnetic properties of rock salt oxides.[14−16] Size-controlled MnO nanocrystals with various morphologies and resulting self-assemblies have been fabricated by adjusting reaction environment and kinetics parameters.[17−21] In recent years, some branched nanostructures of MnO such as hexapod-, nanocross-, and dumbbell-shapes have been reported in succession.[22−24] Note that these branched MnO nanocrystals exhibit a single-crystalline structure. To explain the formation of such novel branched MnO nanocrystals, two distinct mechanisms including the growth/etching mechanism[22] and the oriented attachment mechanism[23,24] have been proposed. As we know, many functional materials (for instance $NiSe_2$, PbS, Cu_2O, and so on) having cubic crystal structures also can form similar single-crystalline branched structures.[25−29] Hence, it is of a great significance to shed light on the formation of such branched single-crystalline nanocrystals by using MnO as a typical model.

In this paper, we successfully synthesized six-horn-like branched MnO nanocrystals by thermal decomposition of $Mn(CH_3CO_2)_2 \cdot 4H_2O$ in the present of 1-octylamine/oleic acid at 400 °C for 30 min. Scanning electron microscopy (SEM) and transmission electron microscopy (TEM) observation indicates that every horn of the six-horn-like MnO nanocrystals is constructed with a bundle of nanorods grown along the [100] direction. Adequate evidence provided by time- and temperature-dependent experiments demonstrates that the formation of such branched MnO can be divided into two processes, i.e., the formation of octahedron-based MnO exposed with polar surfaces and sequent directional etching. In this mechanism, the mixed solvent consisting of organic amine and carboxylic acid plays different roles at two stages of the formation of such novel single-crystalline brached MnO nanostructures.

2. Experimental Section

Chemicals. 1-Butylamine (99%), 1-heptylamine (99%), 1-octylamine (99%), oleic acid (OA, 90%), and manganese acetate ($Mn(CH_3CO_2)_2 \cdot 4H_2O$) were purchased from Alfa Aesar. All reagents were used directly without any further purification.

Syntheses. Six-horn-like branched MnO was synthesized by thermal decomposition of $Mn(CH_3CO_2)_2 \cdot 4H_2O$ in the mixed solvent of organic amine and carboxylic acid, which is based on our previous work with minor modification.[30] In a typical synthesis, 0.66 mL of OA and 3.0 mL of 1-octylamine were mixed to form a transparent solvent at room temperature. Then 0.167 g of $Mn(CH_3CO_2)_2 \cdot 4H_2O$ was added to the solvent and thoroughly dissolved under intense ultrasonic treatment. The resulting brown solution was transferred into a glass tube with a length of 40 cm, and was directly placed in a vertical tube furnace that was already preheated to 400 °C. After the reaction for 30 min, the tube was taken out from the hot tube furnace and instantly added with some ethanol. Finally, green products were collected by high-speed centrifugation. To explore the formation mechanism of the six-horn-like branched MnO, a

* Corresponding author. E-mail: zxxie@xmu.edu.cn and qkuang@xmu.edu.cn. Fax: +86-592-2183047. Tel: +86-592-2180627.

10.1021/jp8092836 CCC: $40.75
Published on Web 01/21/2009

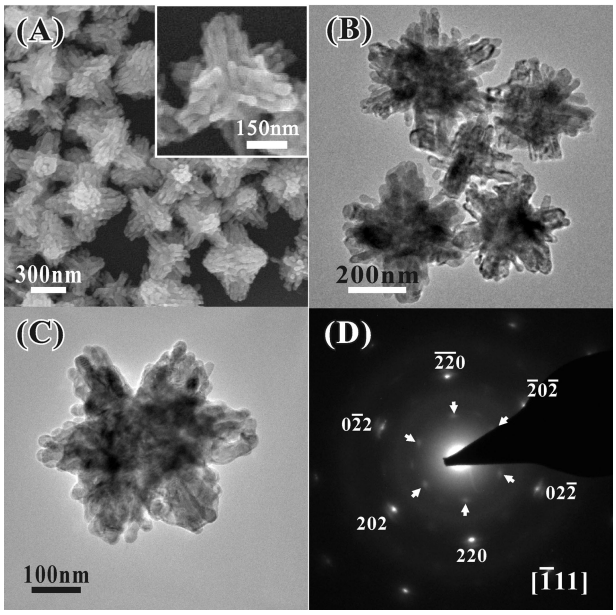

Figure 1. Typical low-magnification (A) SEM image and (B) TEM image of as-prepared six-horn-like branched MnO nanostructures through the decomposition of $Mn(CH_3CO_2)_2 \cdot 4H_2O$ in the mixed solvent of 0.66 mL of OA and 3.0 mL of 1-octylamine at 400 °C for 30 min. (C) TEM image and (D) corresponding SAED image of an individual six-horn-like branched MnO nanostructure.

series of check experiments were further carried out through changing the reaction temperature from 320 to 400 °C, altering the reaction time from 5 to 90 min, and using other different species of organic amine.

Characterization. The composition and phase of as-prepared products were acquired by the powder X-ray diffraction (XRD) pattern, using a Panalytical X-pert diffractometer with Cu Kα radiation. The morphology and crystal structure of as-prepared products were observed by scanning electron microscopy (SEM, Leo 1530) and high-resolution transmission electron microscopy (HRTEM, JEM 2100) with an acceleration voltage of 200 kV. All TEM samples were prepared from depositing a drop of diluted suspensions in ethanol on a carbon film coated copper grid.

3. Results and Discussion

Figure 1A is a typical SEM image of as-prepared products through the decomposition of $Mn(CH_3CO_2)_2 \cdot 4H_2O$ in the mixed solvent of 0.66 mL of OA and 3.0 mL of 1-octylamine at 400 °C for 30 min. It can be found that the products are high-yield branched MnO nanostructures and the size of the whole body ranges from 300 to 500 nm. The corresponding high-magnification SEM image (inset of Figure 1A) reveals that these branched MnO nanostructures have six horns and every horn is constructed with a bundle of nanorods. The diameter of the nanorods is from 20 to 30 nm and the length is about 100−200 nm. More details about the structure of branched MnO nanostructures are provided by related TEM observation. As shown in Figure 1B, almost all nanorods in the same horn grow along the same direction although some slight splits are observed between them. Interestingly, the selective area electron diffraction (SAED) pattern (Figure 1D) taken from an individual branched MnO nanostructure shown in Figure 1C presents one set of diffraction spots projected from the [$\bar{1}$11] zone axis of cubic MnO, displaying that the whole six-horn-like branched MnO nanostructure is a single crystal and each horn grows along the [100] direction. In addition, some additional weak diffraction spots marked by the arrows are also observed in the SAED pattern. According to previous studies,[31] these additional weak diffraction spots should be attributed to the formation of spinel structured Mn_3O_4 (i.e., s-Mn_3O_4) on the surface of MnO in ambient air.

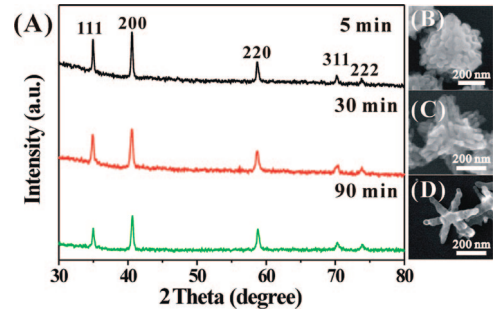

Figure 2. (A) XRD patterns of MnO nanostructures synthesized at 400 °C for different reaction times, i.e., 5, 30, and 90 min. (B−D) Corresponding typical SEM images of the products.

As far as we know, analogous single-crystalline branched MnO structures such as multipods have been prepared via thermal decomposition of various manganese salts in the trioctylamine/oleic acid (TOA/OA) media.[22,23] Different from the above-mentioned MnO branched nanostructures, every horn of as-synthesized six-horn-like branched MnO nanostructures in our study is built up by a bundle of nanorods 20−30 nm in diameter. To shed light on the formation mechanism of our six-horn-like branched MnO nanostructures, several series of experiments were designed and carried out.

First, we tracked the time-dependent growth process of six-horn-like branched MnO nanostructures synthesized at 400 °C by XRD analysis and SEM observation. Figure 2A shows typical XRD patterns of the as-prepared products at 400 °C for 5, 30, and 90 min, respectively. All the patterns can be indexed to the face-centered cubic (fcc) MnO with a rock salt structure ($Fm\bar{3}m$, ICDD 01-075-1090) with lattice constants of $a = 0.4460$ nm. In addition, the widths of the diffraction peaks become broader with the increasing reaction time, which is associated with a gradual decrease of the crystallite size of the products. Panels B−D of Figure 2 are corresponding SEM images of the as-prepared products obtained at 400 °C for different reaction times. At the early stage of the reaction (5 min, Figure 2B), the products are MnO octahedral crystals with a rough surface constructed with 40−60 nm nanoparticles, and the size of the whole octahedral structures ranged from 400 to 500 nm. With the process of the reaction, single-crystalline six-horn-like branched MnO comes into being and its horns are constructed with multirods with a diameter of 20−30 nm (Figure 2C). When the reaction lasts for 90 min, the main morphology of the products are still six-horn-like branched MnO but each horn of such branched MnO nanostructures is just one nanorod with a diameter of about 30 nm. This time-dependent morphology evolution of the products is consistent with the change of the peak width of the corresponding XRD patterns. At the same time, the evolution of the products from octahedral MnO to multipod-like MnO along with reaction time suggests that the formation of six-horn-like branched MnO should follow the growth/etching mechanism, rather than the oriented attachment mechanism proposed by Zitoun et al.[23−25]

This result led us to consider the possibility that octahedral MnO is the parent structure of six-horn-like MnO nanostructures resulting from etching of the mixed solvent of 1-octylamine/OA. To catch the primal morphology (or shape) of the parent

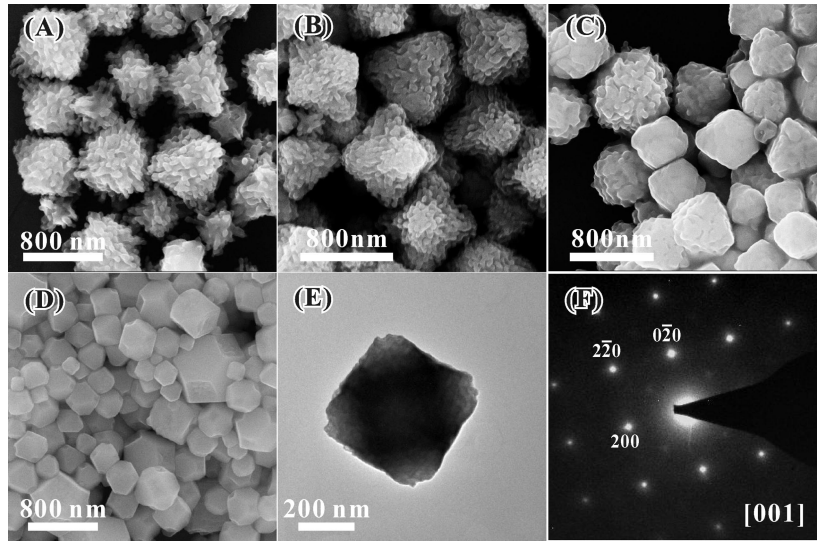

Figure 3. Low-magnification SEM images of the products synthesized at the reaction temperature of (A) 380, (B) 370, (C) 360, and (D) 320 °C for the same reaction time (30 min); (E) TEM image and (F) corresponding SAED pattern of a individual octahedron-based MnO in the products obtained at 320 °C for 30 min.

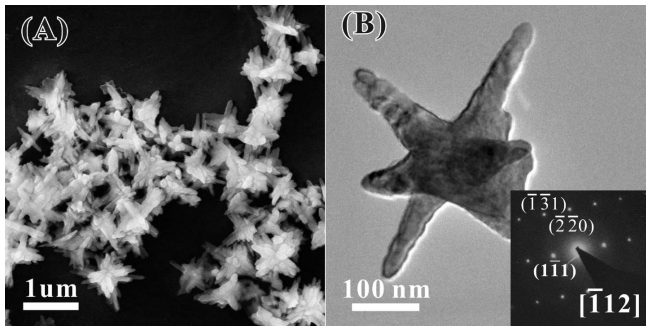

Figure 4. (A) Low-magnification SEM image and (B) TEM image of six-horn-like MnO nanostructures synthesized by refluxing octahedral MnO shown in Figure 3D in the mixed solvent of 3.0 mL of 1-octylamine and 0.66 mL of OA at 400 °C for 30 min. The inset is the corresponding SAED pattern of the individual six-horn-like MnO.

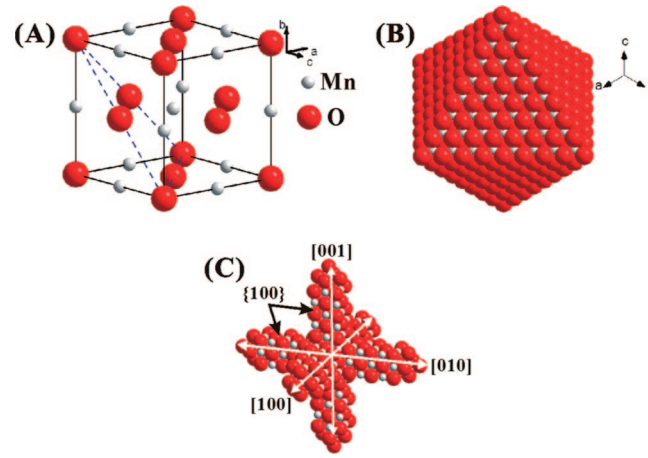

Figure 5. Schematic model of (A) a MnO unit cell, (B) a MnO octahedron, and (C) a six-horn-like MnO.

structure, some contrast experiments were further carried out at lower temperature because lower reaction temperature maybe slow down the etching rate. Panels A−D of Figure 3 are typical low-magnification SEM images of the MnO products obtained at 380, 370, 360, and 320 °C for the same reaction time (30 min), respectively. When reaction temperature is controlled to 380 °C, the outline of the octahedral shape can be identified although many nanorods already form on the surface of the MnO due to the etching action of the 1-octylamine/OA mixed solvent. With the decrease of reaction temperature, the outline of the octahedral shape of MnO is clearer, and accordingly their surface becomes smoother. We find that the morphology of the products obtained at 320 °C for 30 min is well-defined integrated octahedron or inner-truncated octahedron as shown in Figure 3D. These octahedron-based MnO have a smooth surface and their sizes are in the range of 300−700 nm. According to the statistic result from SEM observation, the proportion of inner-truncated octahedron is up to 80%. The corresponding SAED pattern (Figure 3F) taken from the individual MnO inner-truncated octahedron shown in Figure 3E indicates that these octahedron-based MnO are single-crystallized. It should be noted that the surface of octahedron-based MnO is still relatively smooth even if the reaction time is prolonged to 90 min (not shown in this paper). This result indicates that the etching rate at 320 °C is so slow that the primal shape (i.e., integrated octahedron or inner-truncated octahedron) of the MnO parent structure can be successfully reserved in the 1-octylamine/OA mixed solvent.

To further demonstrate that six-horn-like branched structures are evolved from the octahedron-based shape of MnO via an etching process, some MnO octahedral particles obtained at 320 °C for 30 min were again refluxed in the mixed solvent of 1-octylamine/OA at 400 °C. As shown in Figure 4A, six-horn-like MnO nanostructures were finally obtained when octahedron-based MnO were refluxed in the mixed solvent for 30 min. It can be seen that every horn of these branched MnO nanostructures consists of MnO nanorods with a diameter of 30 nm and the whole structure also shows single-crystalline as shown in Figure 4B. This experimental result directly demonstrates that octahedron-based MnO is the parent structure of MnO branched nanostructures. Combining the above experiment results together, we believe that as-synthesized six-horn-like branched MnO nanostructures are evolved from octahedron-based MnO through a selective (or a directional) etching process. In this mechanism, the formation of six-horn-like branched MnO nanostructures can be divided into two stages. First, specific MnO crystals with octahedral shape are formed through the

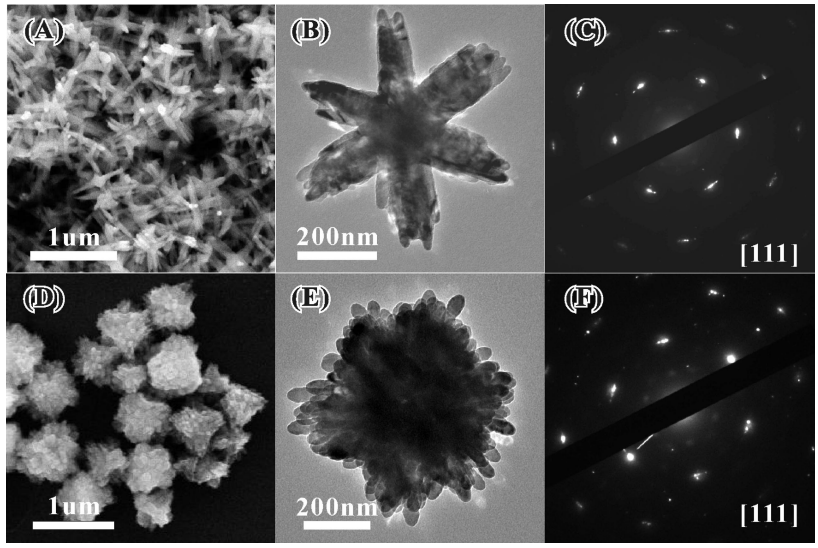

Figure 6. Low-magnification SEM images, TEM images, and SAED patterns of six-horn-like MnO nanostructures synthesized by refluxing octahedral MnO in the mixed solvent of (A−C) 3.0 mL of 1-heptylamine and 0.66 mL of OA or (D−F) 3.0 mL of 1-butylamine and 0.66 mL of OA at 400 °C for 30 min.

decomposition of $Mn(CH_3CO_2)_2 \cdot 4H_2O$ in the mixed solvent of organic amine and carboxylic acid when the temperature of the reaction system rises to 320−360 °C. Second, octahedron-based MnO crystals are gradually etched into branched MnO nanostructures like six-horns by the mixed solvent of organic amine and carboxylic acid when the temperature of the reaction system is in the range of 380−400 °C. In comparison with the second stage (i.e., the etching process), the first stage reaction (i.e., the growing process of octahedron-based MnO) is relatively faster because our experiment has proved that octahedron-based MnO have come into being even in very short reaction times (i.e., 5 min).

Why can the octahedron-based parent structure exposed with {111} faces come into being and be selectively etched in the mixed solvent of organic amine and carboxylic acid? We think that the mixed solvent of organic amine and carboxylic acid play different roles at two stages of the formation of six-horn-like MnO. In the first stage, the electrostatic interaction between negative/positive ions in the mixed solvent and polar planes of rock salt-structured MnO is responsible for the formation of octahedron-like MnO. Structurally, the rock salt structure of MnO is described as a cubic structure where O^{2-} anions are face-cubic-closest (fcc) packed and the Mn^{2+} cations occupy all the octahedral interstices composed by the anions (Figure 5A). Analogous to {0001} and $\{10\bar{1}0\}$ faces of wurtzite-type ZnO,[32] the {111} faces of manganosite-type MnO are also either positively or negatively charged, and the alternate packing of O^{2-} and Mn^{2+} ions results in a normal dipole moment and spontaneous polarization along the ⟨111⟩ directions. Theoretically, rock salt MnO is prone to grow into a cubic shape exposed with nonpolar planes of {100} due to lower surface energy. In our experiments, however, the mixed solvent consisting of carboxylic acid (i.e., OA) and organic amine (i.e., 1-octylamine) can be thought of as one kind of ionic liquid ($R\text{-}COOH + R\text{-}NH_2 \rightarrow R\text{-}COO^- + R\text{-}NH_3^+$), which significantly reduces the surface energy of {111} polar planes through strong electrostatic interaction between the ionic liquid and the polar surfaces. As a consequence, octahedron-based MnO exposed with all {111} polar planes shown in Figure 5B can be synthesized in the mixed solvent of carboxylic acid/organic amine. This is the fundamental reason responsible for the formation of octahedron-based MnO at relatively low reaction temperature (320 °C). For the as-formed octahedron-based parent structure, however, these polarized {111} surfaces are still reactive and have abundant structural defects although they are stabilized by electrostatic interaction to a certain extent. When these octahedron-based MnO remain the mixed solvent, the structural defects on the surface would provide possible sites for sequent directional etching to form a rough surface. With the directional etching process, the nonpolar {100} faces, which are relatively more stable than the {111} faces, are gradually exposed. Because the etching process goes along different channels at the same time, a bundle of nanorods exposed with the {100} faces are formed in the same direction. Finally, the octahedron-based structure would thoroughly transform to the six-horn-like structure. As shown in Figure 5C, every horn of a six-horn-like structure grows along the [100] direction and their side surfaces are surrounded by the {100} faces. From the viewpoint of surface energy, this structure is the most stable in the growth environment of the mixed solvent.

At the directional etching stage, the mixed solvent of organic amine and carboxylic acid as the etching reagent play another crucial role. Previous study has demonstrated the etching action of organic amines for the formation of semiconducting nanocrystals with some special shape.[33] To investigate the influence of organic amine species on the etching process, some octahedron-based MnO as the precursor was again refluxed in the mixed solvent of another organic amine and OA at 400 °C, for example, 1-heptylamine/OA and 1-butylamine/OA. As shown in Figure 6, all octahedron-based MnO are finally transformed into single-crystalline branched MnO nanostructures consisting of many nanorods after the etching process of 30 min whether in the 1-heptylamine/OA solvent (Figure 6A−C) or in the 1-butylamine/OA solvent (Figure 6D−F). However, these experimental results could not establish the validity of the etching action of organic amines because of the presence of OA.

Therefore a series of confirmatory experiments were further conducted by refluxing octahedron-based MnO in the pure 1-octylamine and pure OA at 400 °C for 30 min. As shown in Figure 7A,B, no changes occur in the morphology of octahedron-based MnO that look the same as that before reflux. As shown in Figure 7C,D, on the contrary, the cloudy particle suspension dispersed in OA gradually changed into a bright yellow

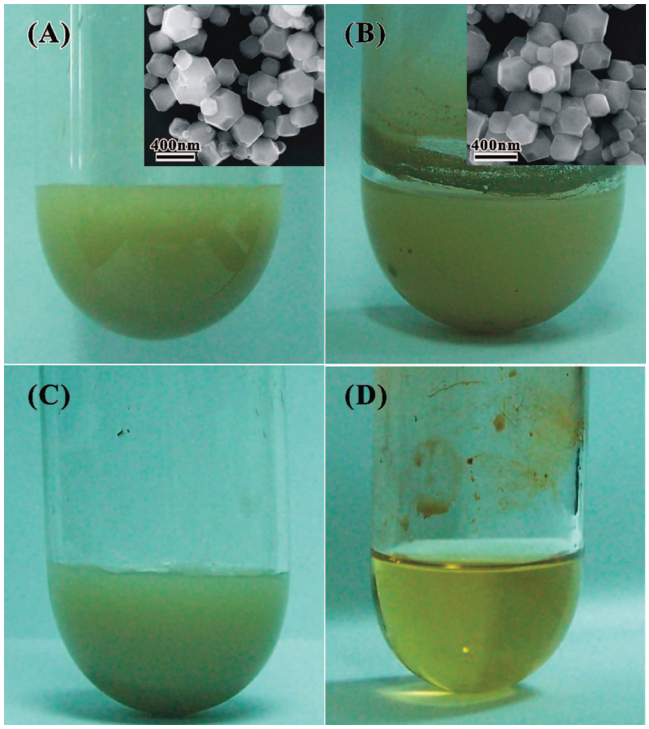

Figure 7. The optical photos of the octahedron-based MnO suspension before and after refluxed in (A, B) 3 mL of 1-octylamine and (C, D) 3 mL of OA at 400 °C for 30 min. The insets in panels A and B are the corresponding SEM images of octahedron-based MnO particles before and after reflux in the pure 1-octylamine.

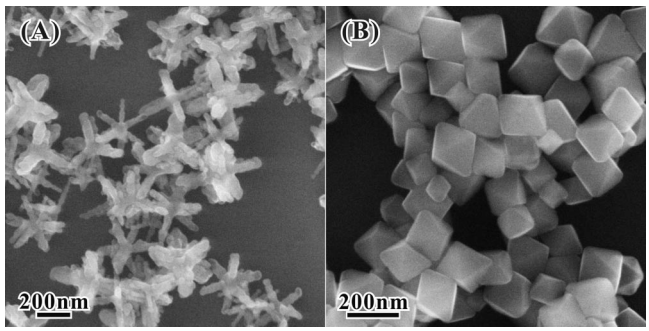

Figure 8. Typical SEM images of MnO particles with various morphologies obtained at different reaction temperature by adjusting the composition proportion of the mixed solvent. (A) Six-horn-like MnO obtained from the mixed solvent of OA (1.32 mL) and 1-octylamine (3 mL) at 400 °C for 30 min; (B) well-defined integrated MnO octahedral obtained from the mixed solvent of OA (0.33 mL) and 1-octylamine (3 mL) at 320 °C for 30 min.

transparent solution when the octahedron-like MnO was refluxed in pure OA at 400 °C for 30 min. This result means that OA rather than organic amine is the real composition acting as the etching reagent due to the formation of dissoluble manganese oleate. Combining all the above results together, we can conclude that the mixed solvent of organic amines and OA provides favorable circumstance for the formation of MnO octahedra exposed with polar surfaces, and OA as the etching reagent is responsible for the evolution from octahedron-based MnO to six-horn-like MnO. The change in the role of the mixed solvent at different formation stages has a close relation with the composition proportion of organic amines and OA in the solvent. As we know, the boiling point (i.e., 286 °C) of OA is obviously higher than that of organic amines (for example, 175 °C for 1-octylamine). At the early stage, the mixture of organic amines and OA presents the ionicity due to the acid−base reaction although organic amine is in excess (n_{OA}:$n_{1\text{-octylamine}}$ = 1:9). But with the volatilization of organic amines, the proportion of OA is larger and larger, which leads to the evolution from octahedron-based MnO to six-horn-like MnO due to the etching action of OA.

On the basis of the above analysis, we propose that the morphology of as-prepared MnO particles obtained at different reaction temperatures can be tuned by adjusting the composition proportion of the mixed solvent. As convincing proof, Figure 8 shows typical SEM images of MnO particles with various morphologies obtained in the mixed solvent with different proportions at the reaction temperatures of 400 and 320 °C. Compared with the six-horn-like MnO consisting of multinanorods shown in Figure 1, most of the as-prepared MnO obtained from the mixed solvent of OA (1.32 mL) and 1-octylamine (3 mL) at 400 °C are also six-horn-like particles but their horns are constructed with a single MnO nanorod. Obviously, the higher the proportion of OA in the mixed solvent is, the more severe the etching degree of MnO is within the same reaction time. In a similar way, high-purity well-defined integrated octahedra of MnO are successfully obtained by decreasing the proportion of OA in the mixed solvent (n_{OA}:$n_{1\text{-octylamine}}$ = 1:18) at 320 °C. As shown in Figure 8B, almost all particles in the products are well-defined integrated MnO octahedra.

4. Conclusion

An unusual form, six-horn-like branched nanostructure of MnO is successfully synthesized by means of the decomposition of $Mn(CH_3CO_2)_2 \cdot 4H_2O$ in the mixed solvent of organic amine and carboxylic acid at 400 °C for 30 min. By changing the reaction time and temperature, we track the evolution process of six-horn-like branched MnO from octahedron-based MnO including integrated octahedron and inner-truncated octahedron, and propose a modified growth/etching mechanism responsible for the formation of branched MnO structures. In this mechanism, the mixed solvent of organic amine and carboxylic acid play the crucial roles, i.e., as an energy-passivating reagent for the formation of octahedron-based MnO exposed with {111} polar surfaces and as a selectively etching reagent for the formation of six-horn-like branched MnO. In addition, the morphology of as-prepared MnO particles obtained at different reaction temperatures is successfully tuned by adjusting the proportion of OA as etching reagent in the mixed solvent. We expect that such a growth/etching mechanism is potentially used for reference to explain the formation of other analogous branched and 3D complex structures.

Acknowledgment. This work was supported by the National Natural Science Foundation of China (Grant Nos. 20725310, 20721001, 20673085, and 20801045) and the National Basic Research Program of China (Grant Nos. 2007CB815303 and 2009CB939804).

References and Notes

(1) Wang, D. L.; Qian, F.; Yang, C.; Zhong, Z. H.; Lieber, C. M. *Nano Lett.* **2004**, *4*, 871.
(2) Dick, K. A.; Deppert, K.; Larsson, M. W.; Martensson, T.; Seifert, W.; Wallenberg, L. R.; Samuelson, L. *Nat. Mater.* **2004**, *3*, 380.
(3) Jung, Y. W.; Ko, D. K.; Agarwal, R. *Nano Lett.* **2007**, *7*, 264.
(4) May, S. J.; Zheng, J. G.; Wessels, B. W.; Lauhon, L. J. *Adv. Mater.* **2005**, *17*, 598.
(5) Mathur, S.; Barth, S. *Small* **2007**, *3*, 2070.
(6) Ding, Y.; Wang, Z. L.; Sun, T. J.; Qiu, J. S. *Appl. Phys. Lett.* **2007**, *90*, 153510.

(7) Hu, J. Q.; Bando, Y.; Golberg, D. *Small* **2005**, *1*, 95.
(8) Manna, L.; Milliron, D. J.; Meisel, A.; Scher, E. C.; Alivisatos, A. P. *Nat. Mater.* **2003**, *2*, 382.
(9) Chen, M.; Xie, Y.; Lu, J.; Xiong, Y. J.; Zhang, S. Y.; Qian, Y. T.; Liu, X. M. *J. Mater. Chem.* **2002**, *12*, 748.
(10) Li, Y. C.; Zhong, H. Z.; Li, R.; Zhou, Y.; Yang, C. H.; Li, Y. F. *Adv. Funct. Mater.* **2006**, *16*, 1705.
(11) Zhou, J.; Ding, Y.; Deng, S. Z.; Gong, L.; Xu, N. S.; Wang, Z. L. *Adv. Mater.* **2005**, *17*, 2107.
(12) Ding, Y. S.; Shen, X. F.; Gomez, S.; Luo, H.; Aindow, M.;.; Suib, S. L. *Adv. Funct. Mater.* **2006**, *16*, 549–555.
(13) Zhang, T. R.; Dong, W. J.; Keeter-Brewer, M.; Konar, S.; Njabon, R. N.; Tian, Z. R. *J. Am. Chem. Soc.* **2006**, *128*, 10960–10968.
(14) Golosovsky, I. V.; Mirebeau, I.; André, G.; Kurdykov, D. A.; Kumzerov, Y. A.; Vakhrushev, S. B. *Phys. Rev. Lett.* **2001**, *86*, 5783.
(15) Nayak, S. K.; Jena, P. *J. Am. Chem. Soc.* **1999**, *121*, 644.
(16) Solovyev, I. V. *Phys. Rev. B* **1998**, *58*, 15496.
(17) Seo, W. S.; Jo, H. H.; Lee, K.; Kim, B.; Oh, S. J.; Park, J. T. *Angew. Chem., Int. Ed.* **2004**, *43*, 1115.
(18) Yin, M.; O'Brien, S. *J. Am. Chem. Soc.* **2003**, *125*, 10180.
(19) Djerdj, I.; Arcon, D.; Jaglicic, Z.; Niederberger, M. *J. Phys. Chem. C* **2007**, *111*, 3614.
(20) Jana, N. R.; Chen, Y. F.; Peng, X. G. *Chem. Mater.* **2004**, *16*, 3931.
(21) Wang, N.; Guo, L.; He, L.; Cao, X.; Chen, C. H.; Wang., R. M.; Yang, S. H. *Small* **2007**, *3*, 606.
(22) Ould-Ely, T.; Prieto-Centurion, D.; Kumar., A.; Guo, W.; Knowles, W. V.; Asokan, S.; Wong, M. S.; Rusakova., I.; Luttge, A.; Whitmire, K. H. *Chem. Mater.* **2006**, *18*, 1821.
(23) Zitoun, D.; Pinna, N.; Frolet, N.; Belin, C. *J. Am. Chem. Soc.* **2005**, *127*, 15034.
(24) Zhong, X. H.; Xie, R. G.; Sun, L. T.; Lieberwirth, I.; Knoll, W *J. Phys. Chem. B* **2006**, *110*, 2.
(25) Du, W. M.; Qian, X. F.; Niu, S. H.; Gong, Q. *Cryst. Growth Des.* **2007**, *7*, 2733.
(26) Qiao, Z. P.; Zhang, Y.; Zhou, L. T.; Xire, Q. *Cryst. Growth Des.* **2007**, *7*, 2394.
(27) Zhou, G. J.; Lü, M. K.; Xiu, Z. L.; Wang, S. F.; Zhang, H. P.; Zhou, Y. Y.; Wang, S. M. *J. Phys. Chem. B* **2006**, *110*, 6543.
(28) Zhao, N.; Qi, L. M. *Adv. Mater.* **2006**, *18*, 359.
(29) Wang, D. B.; Mo, M. S.; Yu, D. B.; Xu, L. Q.; Li, F. Q.; Qian, Y. T. *Cryst. Growth Des.* **2003**, *3*, 717.
(30) Zhou, X.; Xie, Z, X.; Jiang, Z. Y.; Kuang, Q.; Zhang, S. H.; Xu, T.; Huang, R. B.; Zheng, L. S. *Chem. Commun.* **2005**, 5572.
(31) Rusakova, I.; Ould-Ely, T.; Hofmann, C.; Prieto-Centurio'n, D.; Levin, C. S.; Halas, N. G.; Lüttge, A.; Whitmire, K. H. *Chem. Mater.* **2007**, *19*, 1369.
(32) Wang, Z. L. *J. Phys.: Condens. Mater.* **2004**, *16*, 829.
(33) Li, R. F.; Lee, J.; Yang, B. C.; Horspool, D. N.; Aindow, M.; Papadimitrakopoulos, F. *J. Am. Chem. Soc.* **2005**, *127*, 2524.

JP8092836